Am J Transl Res 2020;12(6):2968-2983
www.ajtr.org /ISSN:1943-8141/AJTR0104273

Original Article

4SC-202 induces apoptosis in myelodysplastic syndromes and the underlying mechanism

Weili Wang[1], Zhaoyuan Zhang[2,3,5], Xingyi Kuang[2,3,5], Dan Ma[2,3,5], Jie Xiong[2,3,5], Tingting Lu[2,3,5], Yaming Zhang[2,3,5], Kunling Yu[1,2], Siyu Zhang[1,2], Jishi Wang[2,3,5], Qin Fang[4]

[1]Department of Pharmacy, Guizhou Medical University, Guiyang, P. R. China; [2]Guizhou Province Hematopoietic Stem Cell Transplantation Center, Departments of [3]Hematology, [4]Pharmacy, The Affiliated Hospital of Guizhou Medical University, Guiyang, P. R. China; [5]Key Laboratory of Hematological Disease Diagnostic Treat Centre of Guizhou Province, Guiyang, P. R. China

Received October 31, 2019; Accepted March 21, 2020; Epub June 15, 2020; Published June 30, 2020

Abstract: Epigenetic modifications play crucial roles in regulating the self-renewal and differentiation of hematopoiesis. 4SC-202, a novel inhibitor of histone lysine-specific demethylase 1 (LSD1) and class I histone deacetylases (HDACs), is a potential therapeutic agent to treat myelodysplastic syndrome (MDS). However, it remains unclarified of the mechanism of 4SC-202. In the study, we found that 4SC-202 treatment could inhibit cell viability, induce apoptosis and cause G2/M cell cycle arrest in MDS cell line SKM-1. Heme oxygenase-1 (HO-1) was correlated with disease progression and chemotherapy resistance. Here, we reported that 4SC-202 could down-regulate the expression of HO-1, and up-regulation of HO-1 could significantly attenuate the 4SC-202-induced apoptosis in SKM-1 cells. In addition, the activation of NF-κB pathway was suppressed by 4SC-202, while up-regulation of HO-1 significantly weakened the 4SC-202-induced suppression of the NF-κB pathway, thereby attenuating the efficacy of 4SC-202. However, down-regulation of HO-1 enhanced the sensitivity of 4SC-202 against SKM-1 cells. Moreover, SKM-1 cells were transfected with HO-1 overexpression lentivirus, subsequently injected into the tail vein of NOD/SCID mice, followed by administration of 4SC-202 in mice. As a result, up-regulation HO-1 could partially attenuate 4SC-202-suppressed MDS cells growth in NOD/SCID mice. In conclusion, 4SC-202 could induce apoptosis via the NF-κB pathway, and our present finding may provide a novel therapeutic strategy for MDS.

Keywords: 4SC-202, human histone lysine-specific demethylase 1 (LSD1), class I HDACs, heme oxygenase-1 (HO-1), myelodysplastic syndrome (MDS), NF-κB pathway, apoptosis

Introduction

Myelodysplastic syndrome (MDS) is a clonal disease of pathological hematopoiesis, which can be easily transformation into acute myeloid leukemia (AML). MDS is mainly characterized by the presence of peripheral cytopenia, accumulation of primary cells, dysplastic hematopoietic differentiation, but lacks the characteristics of acute leukemia. Currently, conventional chemotherapy can relieve cytopenia, improve quality of life and delay disease progression, however, MDS patients are threatened by poor prognosis in the case of chemotherapy resistance. Despite the long-term survival in 30%-40% MDS patients via allogeneic hematopoietic stem cell transplantation (allo-HSCT), most MDS patients are elderly and allo-HCST itself causes serious complications and mortality [1]. Therefore, it is urgently required to explore feasible therapeutic approaches in MDS in clinical practice. Epigenetic modifications play crucial roles in regulating the self-renewal and differentiation of hematopoiesis, which are also the main oncogenic cause of MDS and AML. Over the past decade, several epigenetic regulators have been developed and assessed in preclinical and clinical studies. In addition to hypomethylating agents in this category, inhibitor of the human histone lysine-specific demethylase 1 (LSD1) is considered as the most promising epigenetic approach ameliorating MDS and AML, which invokes the myeloid development programs [2-4]. The overexpression of LSD1 has been reported in approximately 60% of MDS patients [2]. In a spectrum of LSD1 inhibi-

tors combined with conventional chemotherapy agents, LSD1 inhibitors reactivate myeloid differentiation in AML and MDS cells that are not spontaneously susceptible to chemotherapy, but hardly affect normal hematopoietic stem cells [5]. Moreover, LSD1 has been reported to block myeloid maturation and to promote malignant hematopoiesis and the development and reproduction of leukemia [6-8], which is an extremely safe strategy for regeneration of normal hematopoiesis stem cells.

LSD1, also known as KDM1A, AOF2 or BHC110, is the first discovered histone demethylase and mainly acts on histone 3 lysine 4 methylation 1/2 (H3K4me1/2) and histone 3 Lysine 9 methylation (H3K9me1/2) [9]. H3K4 methylation is a hallmark of active transcription, while H3K4 demethylation acts as a transcriptional co-repressor [5]. Among them, H3K4me2 is a marker for both activity enhancer and promoter [10]. LSD1 is involved in different complexes to promote H3K4 demethylation and to form chromatin into an inhibitory conformation, such as a CoREST transcriptional repressor complex composed of LSD1 and histone deacetylase 1/2 (HDAC1/2). LSD1 is abnormally blind to super-suppressor gene. Silencing LSD1 activates GFI-1, which is identified as the signature of LSD1 super-enhance activation, thereby hindering MDS and MDS-associated leukemia oncogenic programs [3, 11]. GFI-1 can bind with histone deacetylases to trigger transcriptional repression and is associated with HDAC1/2/3. The signal that promotes LSD1 demethylation activity is the local deacetylation marker on histone H3 removed by the LSD1 downstream gene HDAC1/2 [12-14]. HDAC removes acetyl groups from lysine in histones, thereby repressing DNA transcription [15]. Co-treatment of LSD1 antagonist and HDACs inhibitor could significantly improve the survival of mice engrafted with human AML cells, without any toxicity [14]. Targeting the CoREST complex with dual HDACs and LSD1 inhibitors is also effective by slowing tumor cell growth in a melanoma mouse xenograft model [16]. Therefore, we postulated that co-inhibition of LSD1 and HDACs would synergistically activate repressed genes, thereby inducing apoptosis and causing cell cycle arrest in MDS cells.

4SC-202 is a novel oral benzamide type of LSD1 and class I HDACs inhibitor (HDAC1/2/3) [17]. 4SC-202 has been evaluated in phase I clinical trials in patients with advanced hematologic malignancies including MDS, which has revealed that 4SC-202 is safe, well tolerated and has good anti-tumor activity [18]. In addition, the action mechanism of 4SC-202 has been recently elucidated in cutaneous T cell lymphoma cells [19]. However, the mechanism remains unclear in MDS cells. Overexpression of heme oxygenase-1 (HO-1) has been documented in hematological malignancies, which is also correlated with disease progression and chemotherapy resistance [20-22]. Indeed, HO-1 is highly expressed in MDS and clearly associated with MDS risk stratification, and HO-1 silencing enhances the sensitivity of hypomethylate agents against MDS cells both in vitro and in vivo [22, 23]. Our group has previously demonstrated that the expression level of HO-1 is regulated by GFI-1 or HDAC1/2/3 [24-26]. In addition, we have also shown that inhibition of NF-κB pathway could down-regulate the expression of HO-1 in our previous study [27]. Constitutive NF-κB is activated in bone marrow samples from high-risk MDS patients, which plays a crucial role in the transformation of MDS into AML. NF-κB pathway suppression by inhibitor OBY11-7082 or p65 siRNA can rapidly induce apoptosis in MDS cells by up-regulating NF-κB targeting proapoptotic genes, followed by release of caspase activators cytochrome C by mitochondria and activation of caspase-dependent apoptotic genes [28]. LSD1 has also been reported to produce 8-oxoG and to activate transcription factor NF-κB, and targeting LSD1 can inhibit the activation of NF-κB pathway [29, 30]. Therefore, we hypothesized that 4SC-202 induced apoptosis through the NF-κB /HO-1 pathway.

Materials and methods

Reagents and antibodies

4SC-202 was purchased from Med Chem Expression (New Jersey, USA). HO-1 inhibitor Znpp was purchased from Cayman Chemical (Ann Arbor, MI, USA). HO-1 activation Hemin was obtained from Sigma (St. Louis, MO, USA). Anti-LSD1, anti-β-actin, anti-HO-1 and secondary antibodies (HRP-conjugated goat anti-rabbit or anti-mouse) were purchased from MDL biotech (Beijing, China). Primary antibodies against HDAC1/2/3, H3K4me2, cleaved-caspase-3, cl-

Table 1. Characteristics of MDS patients

Patient No.	Karyotype	Age	BM blasts (%)	Cytopenia	IPSS	WHO classification
1	46, XX	39	5.9	2	1	RAEB-1
2	46, XY	65	9	3	1	RAEB-1
3	46, XX	20	7	3	1	RAEB-1
4	46, XY	17	6.99	2	1	RAEB-1
5	46, XX	61	7.80	2	1	RAEB-1
6	46, XY	38	9.39	3	1	RAEB-1
7	46, XX	61	10	2	2	RAEB-1
8	46, XY	75	10.39	2	2	RAEB-1
9	46, XY	85	5.89	3	2	RAEB-2
10	46, XX	41	18.8	3	2	RAEB-2
11	46, XY	49	20	3	2	RAEB-2
12	46, XY	50	8.44	3	2	RAEB-2
13	46, XX	81	12.89	3	2	RAEB-2
14	46, XY	53	11	3	2	RAEB-2
15	46, XY	70	23	3	NA	RAEB-t/AML
16	46, XY	51	4.81	2	NA	RAEB-t/AML
17	46, XY	55	23	3	NA	RAEB-t/AML
18	46, XY	57	76	2	NA	RAEB-t/AML
19	46, XX	36	21.72	3	NA	RAEB-t/AML
20	46, XY	63	34	3	NA	RAEB-t/AML
21	46, XY	54	39	3	NA	RAEB-t/AML
22	46, XY	48	22	3	NA	RAEB-t/AML
23	46, XY, t (9;22)	61	10	3	2	RAEB-2
24	46, XX, t [8;2]	30	15	3	2	RAEB-2
25	47, XX, +der (5)	25	8	3	1.5	RAEB-1
26	47, XY, +8	68	8.9	2	1.5	RAEB-1
27	46, XY, del (5q)	77	45.97	3	NA	RAEB-t/AML
28	45, XX, -7	73	6	3	2	RAEB-1
29	45, XY, -7	76	13.31	3	3	RAEB-2
30	45, XY, -7	77	29	3	NA	RAEB-t/AML
31	Complex	85	13	3	3	RAEB-2
32	complex	81	16.51	3	3	RAEB-2

RAEB, refractory anemia with excess of blasts (5-9% BM blasts RAEB-1, 10-19% BM blasts RAEB-2); RAEB-transform AML (RAEB-t/AM); NA, not applicable.

eaved-caspase-9, p21, CDK1, AC-H3, BCL-2, BAX were bought from Santa Cruz (Heidelberg, Germany). And antibodies p-p65^{S536} and p-IκB-α$^{S32/S36}$ were bought from Cell Signaling Technology (Beverly, MA, USA).

Clinical samples

Bone marrow samples were obtained from newly diagnosed MDS patients and MDS transforming AML patients and from healthy individuals in the Affiliated Hospital of Guizhou Medical University as well as all specimens were collected after written informed consent according to the Declaration of Helsinki. These patients were diagnosed of using WHO Classification in **Table 1**. Bone marrow mononuclear cells were separated from by Ficoll (Solarbio, Beijing, China) gradient centrifugation. This study was approved by the institutional review bo-ard of The Affiliated Ho-spital of Guizhou Medical University.

Immunocytochemistry

Bone marrow mononuclear cells were rinsed in PBS and fixed by incubation with 4% formaldehyde in PBS for 30 min at room temperature. Cells were deparaffinized and pretreated with 10 mM citrate (pH 6.0; Zymed, South San Francisco, CA, USA) in a steam pressure cooker (Decloaking Chamber; BioCare Medical, Walnut Creek, CA, USA) and subsequently washed in distilled water. All further steps were performed at room temperature in a hydrated chamber. Cells were pretreated with Peroxidase Block (Dako USA, Carpinteria, CA, USA) for 5 min to quench endogenous peroxidase activity. Primary anti-HO-1, LSD1 and HDAC3 antibodies were incubated in the Dako diluent (Dako USA) for 1 h. Cells were washed in 50 mM Tris (Tris (hydroxymethyl) aminomethane)-Cl (pH 7.4) and incubated with horseradish peroxidase (HRP)-conjugated antibody solution (Beyotime Institute of Biotechnology, Haimen, China) for 30 min. After further washing, immunoperoxidase staining was developed with the chromogen diaminobenzidine (Dako USA), and cells were coun-

terstained with Harris hematoxylin (Beyotime Institute of Biotechnology, Haimen, China).

Cell culture

The high risk MDS cell line SKM-1 (obtained from the Japanese Collection of Research Bioresources) was cultured in RPMI 1640 (Sigma, USA) medium supplemented with 10% fetal bovine serum (Ausgenex) and 1% penicillin/streptomycin (Invitrogen, Carlsbad, USA) in a 5% CO_2 humidified atmosphere at 37°C.

Cell viability assays

Cells were seeded in 96-well plates, treated with different concentrations of 4SC-202 for 24 or 48 hours, and lastly added 10 μL cell counting kit-8 (CCK-8) assay (Beyotime Institute of Biotechnology, Haimen, China) to every well. After incubator 1 h, absorbance values at 450 nm were measured with UV-1700 ultraviolet spectrophotometer (Shimadzu, Japan).

Apoptosis assay

After incubation with drugs, SKM-1 cells were harvested and washed with normal saline, then double stained with Annexin V-FITC and propidium iodide (7Sea Biotech, Shanghai, China) according to the manufacturer's instructions. Apoptotic cells were measured by FACS calibur flow cytometer (BD Biosciences, San Jose, CA, USA).

Cell cycle analysis

After cells were treated with the drugs, cells were harvested, washed and stained according to the manufacturer's instructions of cell cycle detection kit (7Sea Biotech). DNA count of samples were analyzed by flow cytometer and Multicycle software.

Quantitative real time PCR (qRT-PCR)

Total RNA was extracted from cells using Trizol reagent (Invitrogen), followed by reverse transcription with the use of Revertaid First Strand cDNA Synthesis Kit (Thermo Scientific, Waltham, Massachusetts, USA). Complementary DNAs were detected by using a SYBR Green PCR Master Mix (TianGen Biotech, Beijing, China) on the quantitative real-time PCR using SYBR Green Supermix (Bio-Rad, Hercules, CA). All operations were followed by the manufacturer's instructions. The relative expression of mRNA was calculated according to 2^-CT and β-actin was selected as the internal control.

Western blot analysis

Total protein was isolated by PMSF buffer and IPRA (Solei Bao Technology Co., Ltd., Beijing, China) according to the manufacturer's instructions. Protein samples were loaded and separated by 10% SDS-PAGE gel and subsequently transferred onto PVDF membranes (Millipore Corporation, Milford, MA, USA). The membranes were blocked with 5% nonfat dry milk in Tris-Buffered Saline Tween20 (TBST) for 2 hours and then incubated the primary antibodies for 2 hours. After being washed by TBST, incubated with secondary antibody and washed with TBST again, all protein bands were visualized with using the enhanced chemiluminescence (7Sea Biotech) and lastly detected with Tanon 4200 automatic chemiluminescence image analysis system (Tanon, Shanghai, China). β-actin was used as internal reference.

Knock-down of LSD1 and HDAC3 by small interfering RNA (siRNA)

siRNA against LSD1 and HDAC3 (si-LSD1/si-HDAC3, China Quan Yang Biological Co., Ltd., Shanghai) respectively inhibited LSD1 and HDAC3, and scrambled siRNA (NC) was used as a negative control. Cells were transfected with siRNA and used transfection reagent of Lipo6000™ (Beyotime Biotechnology, Shanghai, China) according to the manufacturer's instructions. qRT-PCR was used to detect the silencing of LSD1or HDAC3 expression.

Immunofluorescence staining

The p65 was examined by immunofluorescence. SKM-1 cells were plated on 6-well culture plates, Hemin or Znpp pretreated or left untreated for 1 hour, incubated with 4SC-202. Then the cells were rinsed in PBS and fixed by incubation with 4% formaldehyde in PBS for 30 min at room temperature. After washing with PBS, cells were permeabilized with PBS containing 0.25% Triton X-100. The cells were blocked in PBS containing 5% BSA for 30 min. Next, with further washing, cells were incubated with a rabbit anti-P65 monoclonal antibody for 24 hours at 4°C. After washing with PBS, cells were incubated with FITC-conjugated goat

anti-rabbit antibody (1:200) for 1 hour. Then, the nucleus was stained with DAPI (4,6-diamidino-2-phenylindole) and cells were photographed by fluorescent microscopy.

Construction of recombinant lentiviral vectors and transfection

Self-prepared recombinant lentivirus-V5-D-TOPO-HO-1-EGFP(LV-HO-1) and its' control vector lentivirus-V5-D-TOPO-EGFP(EV) were cotransfected into 293FT packaging cell line. After the infection according to the manufacturer's instructions, the positivity of lentivirus-mediated HO-1 and transduction was observed by fluorescence microscopy and the transfection rates were determined by qRT-PCR.

Xenograft transplantation

Female 5 to 6-week-old NOD/SCID mice were purchased Beijing HEK Bioscience. 5 million SKM-1 cells were a tail vein injection. At 2 weeks post-transplantation, peripheral blood mononuclear cells from the recipient mice were stained with anti-human CD45-PECY7 (BD Biosciences) analyzed with FCM. Only the mice with more than 0.1% human CD45-positive cells in peripheral blood were randomly treated with 4SC-202 (80 mg/kg/day) by oral administration [3, 23]. We divided the successfully transplanted mice into EV or LV-HO-1 mice non-administration groups, EV or LV-HO-1 mice administration groups and the human $CD45^+$ content of the 4SC-202 administrator groups were detected by FCM two weeks after administration. The survival of mice is represented by a Kaplan-Meier plot. All animal experiments were performed in accordance with the National Institutes of Health Guide for the Care and Use of Laboratory Animal and were approved by the Biomedical Ethics Committee of the Affiliated Hospital of Guizhou Medical University.

Statistical analysis

GraphPad Prism 8.0 software (Graphpad Software, Inc, USA) was used to statistically analyze the data. All data are expressed as mean ± standard deviation. Statistical analysis was performed using analysis of variance and t-test. $P<0.05$ was considered statistically significant.

Results

The overexpression of LSD1, HDAC3 and HO-1 in MDS/AML patients

We collected a series of samples from MDS and MDS-transformed AML patients. All patients were diagnosed and classified according to the WHO classification (**Table 1**). To analyze the expression of LSD1, HDAC3 and HO-1 in during MDS progression, these samples were classified into refractory anemia with excess of blasts (RAEB) I/II and RAEB-transform AML (RAEB-t/AM) groups. The mRNA expression level of LSD1 was first detected qRT-PCR (**Figure 1A**), which revealed that mRNA expression level of LSD1 was significantly higher in the RAEBI/II and RAEB-t/AML groups than normal donors ($P<0.01$ and $P<0.001$, respectively). Western blot further revealed that the protein expression level of LSD1 was higher in MDS/AML patients than normal donors overall (**Figure 1B**). Similarly, the expression of HDAC3 gene was detected by the same techniques in the above samples, showing that the expression of HDAC3 was higher in the RAEBI/II and RAEB-t/AML groups than normal donors ($P<0.01$ and $P<0.001$, respectively). Meanwhile, HO-1 gene expression was also detected in the above samples. qRT-PCR analysis showed HO-1 overexpression in the RAEBI/II and RAEB-t/AML groups compared with normal donors ($P<0.05$ and $P<0.001$, respectively), which was further validated by Western blot (**Figure 1A**, **1B**). In addition, the expression of LSD1, HO-1 and HDAC3 in normal donors and patients were observed by immunocytochemistry. We observed higher expression of LSD1, HO-1 and HDAC3 compared to normal donors (**Figure 1C**). Taken together, LSD1, HDAC3 and HO-1 were overexpressed in MDS/AML patients.

4SC-202 affected cell viability, apoptosis and cell cycle in SKM-1 cells

4SC-202 is an inhibitor of LSD1 and class I HDACs (HDAC1/2/3). To investigate the cellular function induced by 4SC-202 in SKM-1 cells, an acute myeloid leukemia cell line was established in the leukemic phase during the progression of MDS to AML (MDS/AML). CCK-8 assay and flow cytometry using propidium iodide or Annexin V-staining were used to asses impact of 4SC-202 on cellular viability, cell

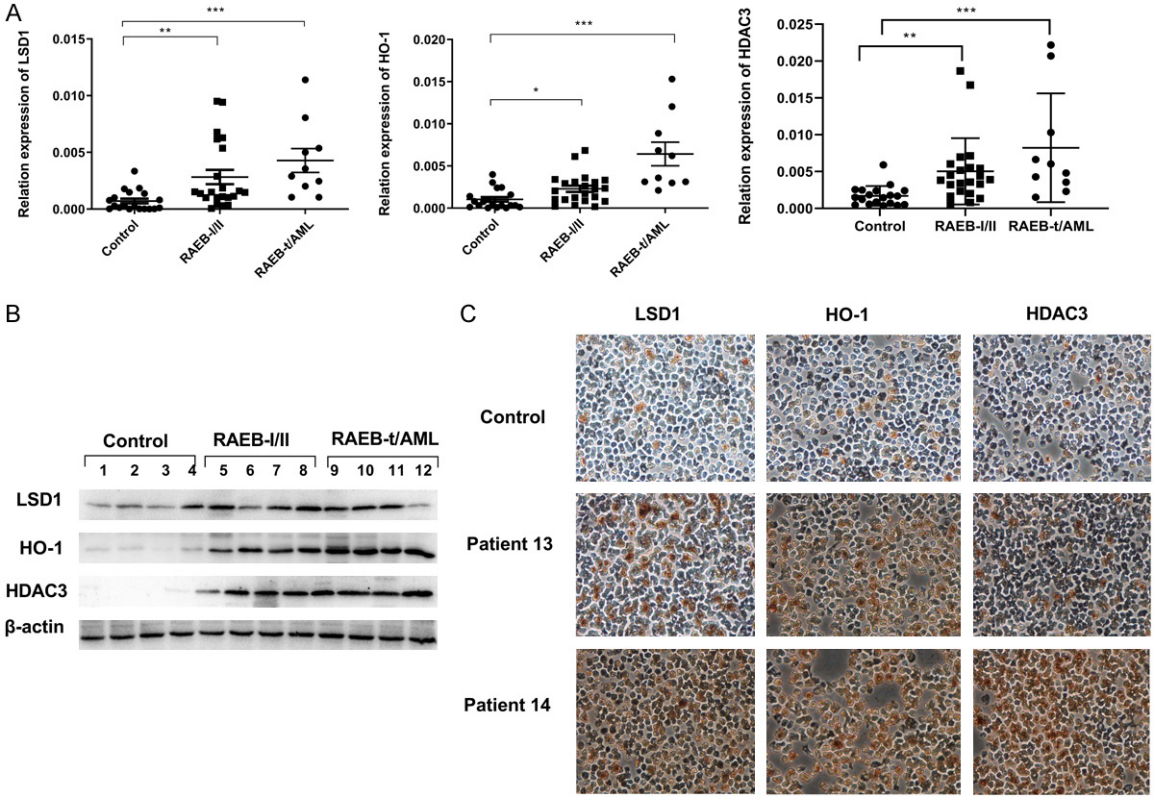

Figure 1. Expression levels of LSD1, HDAC3 and HO-1 in MDS/AML patients. A. qRT-PCR indicated that the mRNA expression levels of LSD1, HDAC3 and HO-1 in MDS/MDS-AML transformed patients were higher expression compared with control (normal donor). Dates were shown as mean ± SD. *, P<0.05; **, P<0.01; ***, P<0.001. Statistical analysis was performed by the student's t test. B. Western blot also determined that the protein levels of LSD1, HDAC3 and HO-1 in MDS/AML patients were overexpression. C. The expression of LSD1, HO-1 and HDAC3 in normal donors and patients were observed by immunocytochemistry. Brown represented the positive cell. Control represented normal donor. β-actin was used as the loading control.

cycle progression and survival. CCK-8 assay was performed to assess SKM-1 cell viability after 4SC-202 treatment. As shown in **Figure 2A**, incubation for 24 or 48 hours affected cells viability in a dose-dependent manner (0-4 μM) (**Figure 2A**). After incubation for 24 hour, flow cytometry showed that 4SC-202 could induce apoptosis in SKM-1 cells in a dose-dependent manner (0, 0.1, 0.3, 0.5, 0.7, 1 μM) (**Figure 2B**, **2C**). Additionally, after incubation for 48 hours under the same drug concentration, flow cytometry showed more obvious cell apoptosis compared with that of 24 hours (**Figure 2D**, **2E**). Then we examined the effects of 4SC-202 on cell cycle progression. As a result, 4SC-202 could cause G2/M cell cycle arrest in a dose-dependent manner (**Figure 2F**, **2G**). Altogether, these results demonstrated that 4SC-202 exerted strong effects against SKM-1 cells through inhibiting cell viability, causing cell cycle arrest in G/M phase and inducing cell apoptosis.

4SC-202 affected the expression of apoptosis- and cell cycle-related proteins and decreased HO-1 in SKM-1 cells

To further analyze the mechanism underlying apoptosis and cell cycle progression, Western blot was used to detect the expression of 4SC-202-related proteins, apoptosis-related proteins and cell cycle-related proteins after exposure with different concentration (0, 0.1, 0.3, 0.5, 0.7, 1 μM) or times (0, 6, 12, 24, 48 h). As a result, 4SC-202 treatment gradually decreased the protein expression of LSD1, HDAC2 and HDAC3 in a dose- and time-dependent manner. After 4SC-202 treatment at a concentration of 0.5 μM for 24 hours, the expression of HDAC1 protein began to decrease. Moreover, acetylated histone 3 (AC-H3) and H3K4me2 expression was markedly increased. The protein expression of BCL-2 and CDK1 was gradually decreased, while BAX, cleaved caspase 3, cleaved caspase 9 and p21 was significantly

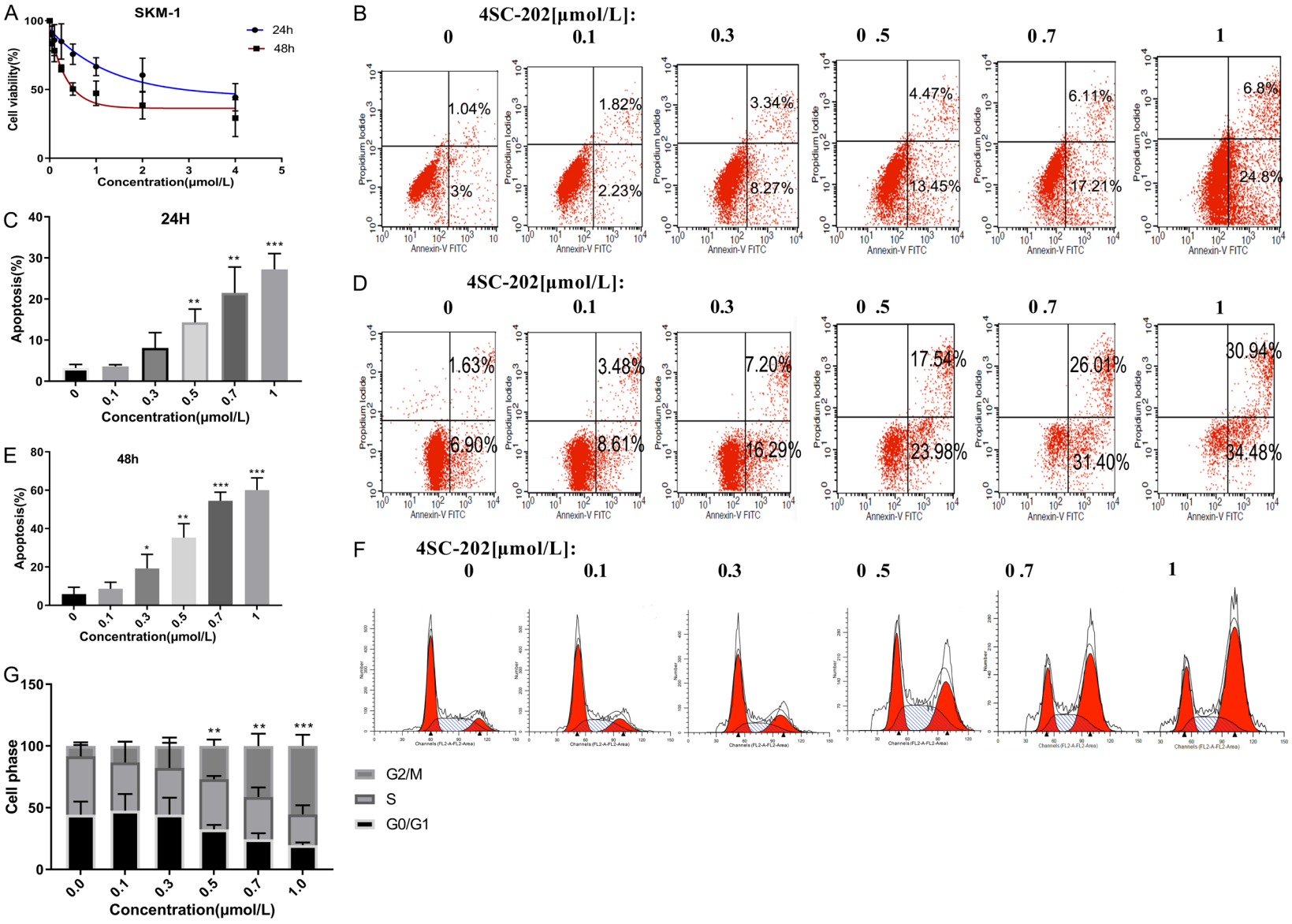

Figure 2. 4SC-202 suppressed cell viability, induced apoptosis and caused cell cycle arrest at G2/M phase in SKM-1 cells. A. Cells were treated with different concentrations of 4SC-202 (0-4 mM) for 24 h and 48 h. The OD values at a wavelength of 450 nm were detected by CCK-8 assay and the dates were analyzed by GraphPad Primer 8. CCK-8 assay indicated that 4SC-202 reduced the growth of SKM-1 cells. B-E. Next, flow cytometry (Annexin V-FITC/PI staining) analysis showed that the apoptotic rates were increased by 4SC-202 in a dose- and time-dependent manner. F, G. SKM-1 cells were exposed to 4SC-202 at the different concentration

for 24 h. Flow cytometry analysis shown that 4SC-202 caused cell cycle arrest at G2/M phase in a dose- dependent manner. All experiments were repeated three times. Dates were shown as mean ± SD. *, P<0.05 versus control; **, P<0.01 versus control; ***, P<0.001 versus control. Statistical analysis was performed by the student's t test.

increased in a concentration- and time-dependent manner, whereas the protein expression of cleaved caspase 3 and cleaved caspase 9 were markedly increased in a dose- and time-dependent manner (**Figure 3A**, **3C**). Meanwhile, the mRNA levels of LSD1 and HDAC3 were detected by qRT-PCR at treatment with different concentrations (0, 0.1, 0.3, 0.5, 0.7, 1 μM) of 4SC-202 for 24 h. After 4SC-202 treatment at a concentration of 0.7 μM for 24 hours, the expression of HDAC3 and LSD1 genes began to decrease (P<0.01; P<0.05, respectively) (**Figure 3B**).

In addition, we also found that 4SC-202 down-regulated the protein level of HO-1 in a time- or dose-dependent manner (**Figure 3D**, **3F**). After 4SC-202 treatment at a concentration of 0.3 μM for 24 hours, the expression of HO-1 gene was markedly decreased (**Figure 3E**). Hence, cells were transfected with HO-1 overexpression lentivirus (LV-HO-1) and its empty vector (EV). Transfection efficiency was subsequently detected by fluorescence microscopy, and the down-regulation level of HO-1 mRNA was measured by qRT-PCR (**Figure 3G**, **3H**). Meanwhile we examined the change of apoptosis-related protein, showing that HO-1 down-regulated the expression of cleaved caspase9 protein, but failed to change the protein levels of cleavage caspase3, Bad, Bcl-2. However, after treatment with 0.5 μM 4SC-202 for 24 h in transfected cells, HO-1 could partially reverse the 4SC-202-induced apoptosis-associated protein levels (**Figure 3I**). Moreover, HO-1 significantly decreased 4SC-202-induced apoptosis rate (P<0.05) (**Figure 3J**, **3K**). Taken together, these data demonstrated that up-regulation HO-1 partially reversed the activity of 4SC-202 in SKM-1 cells.

4SC-202 induced cell apoptosis and decreased HO-1 expression via NF-κB pathway, and HO-1 affected the efficacy of 4SC-202 in SKM-1 cells

Constitutive activation of NF-κB in MDS cells plays a crucial role in activating caspase-dependent apoptotic genes. Hence, after incubation with 4SC-202, Western blot was utilized to detect the expression of phosphorylated p65 (p-p65), phosphorylated IκB-α (p-IκB-α), total p65 and total IκB-α protein. We found that the protein levels of p-p65 and p-IκB-α were significantly decreased in a concentration-dependent pattern, while the protein levels of total p65 and total IκB-α protein remained unchanged (**Figure 4A**). Similarly, treatment with 0.5 μM 4SC-202 for different time (0, 6, 12, 24 and 48 hours), the protein levels of p-IκB-α and p-p65 were gradually decreased in a time-dependent pattern (**Figure 4B**). The translocation of p65 is known to be an important indicator of NF-κB activation. Therefore, treatment with or without 0.5 μM 4SC-202, immunofluorescence staining showed that translocation of p65 to the nucleus was blocked by treatment with 4SC-202 (**Figure 4C**). Collectively, 4SC-202 significantly suppressed the NF-κB pathway.

Moreover, we further elucidated how these cellular functions were caused by 4SC-202. In the study, si-LSD1 was transfected into SKM-1 cells to silence LSD1, followed by determination of knockdown efficiency. SKM-1 cells were treated with si-LSD1 or its empty siRNA (NC siRNA) as a negative control to eliminate the side-effects of transfection or RNA incorporation into cells. After incubation with si-LSD1 or NC siRNA for 48 hours, LSD1 was significantly silenced in the siLSD1 group, which was barely changed in the NC group (**Figure 4D**). Western blot was subsequently used to detect the expression of NF-κB pathway and HO-1 proteins in both NC and si-LSD1 groups, revealing that the protein expression levels of p-p65 and p-IκB-α of NF-κB pathway and HO-1 were significantly down regulated in the si-LSD-1 group than those in the NC group, and similarly the protein levels of total p65 and total IκB-α remained changed (**Figure 4E**). Meanwhile, we also investigated the effects of HDAC1/2/3 on 4SC-202 activity. HDAC1 and HDAC2 are downstream genes of LSD1, thus, cells were transfected with si-HDAC3 to silence HDAC3. We also found that low HDAC3 expression repressed the activation of NF-κB pathway and decreased the expression HO-1 (**Figure 4F**, **4G**). Our previous studies have shown that repressing the activation of NF-κB pathway could down-regulate HO-1 expression [27]. Hence, after transfection with EV and LV-HO-1, cells were treated with or without 4SC-202, followed

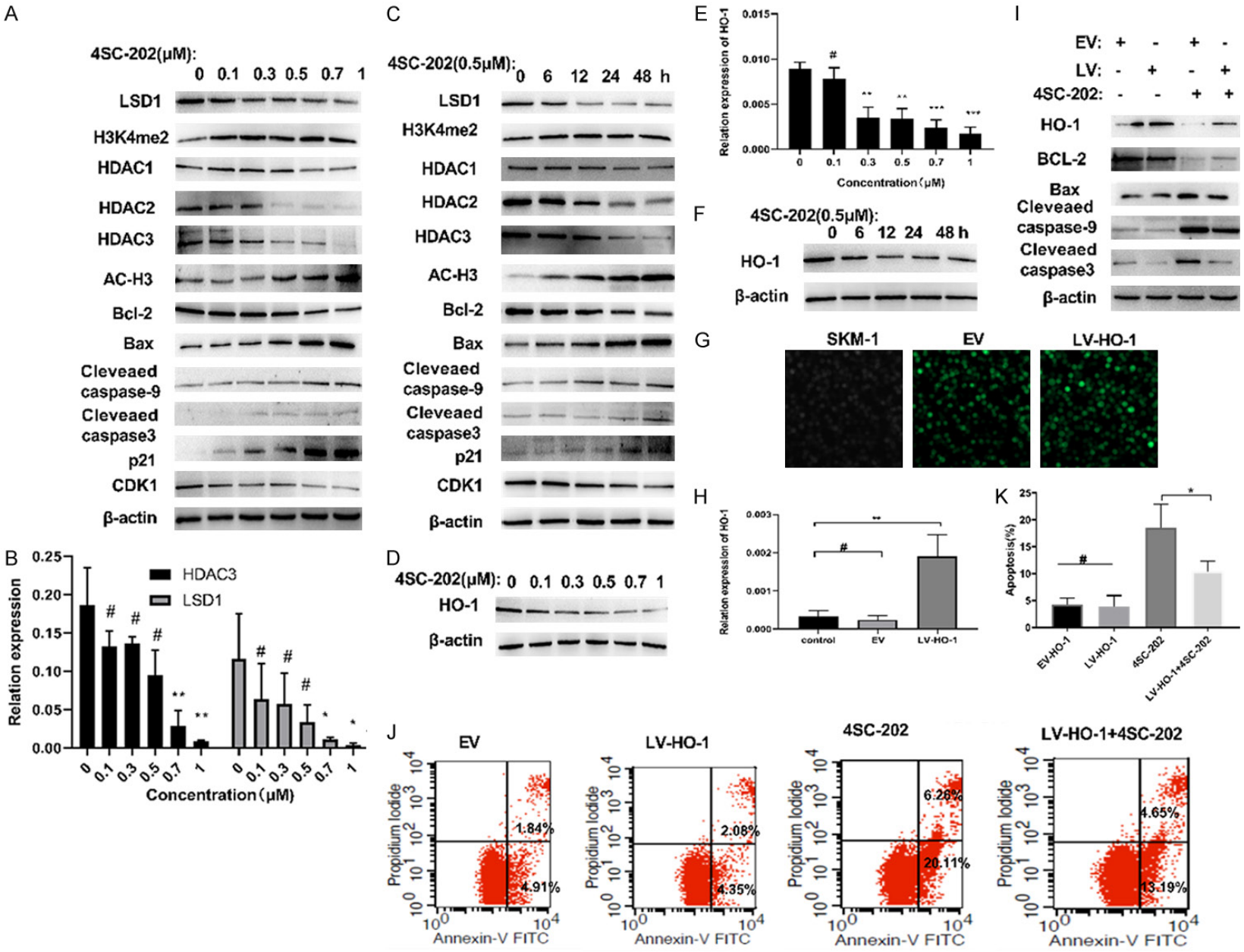
A
4SC-202(μM): 0 0.1 0.3 0.5 0.7 1
LSD1
H3K4me2
HDAC1
HDAC2
HDAC3
AC-H3
Bcl-2
Bax
Cleveaed caspase-9
Cleveaed caspase3
p21
CDK1
β-actin
B
HDAC3
LSD1
Relation expression
Concentration (μM)
C
4SC-202(0.5μM): 0 6 12 24 48 h
D
4SC-202(μM): 0 0.1 0.3 0.5 0.7 1
HO-1
β-actin
E
Relation expression of HO-1
Concentration (μM)
F
4SC-202(0.5μM): 0 6 12 24 48 h
HO-1
β-actin
G
SKM-1
EV
LV-HO-1
H
Relation expression of HO-1
control
EV
LV-HO-1
I
EV:
LV:
4SC-202:
HO-1
BCL-2
Bax
Cleveaed caspase-9
Cleveaed caspase3
β-actin
J
EV
LV-HO-1
4SC-202
LV-HO-1+4SC-202
Propidium Iodide
Annexin-V FITC
1.84%
4.91%
2.08%
4.35%
6.26%
20.11%
4.65%
13.19%
K
Apoptosis(%)
EV-HO-1
LV-HO-1
4SC-202
LV-HO-1+4SC-202

Figure 3. 4SC-202 affected the expression of apoptosis- and cell cycle-related proteins and decreased HO-1 expression in SKM-1 cells. (A) Western blot analyzed that the expression levels of LSD1, HDAC1/2/3, BCL-2 and CDK1 proteins were decreased and the expression levels of H3K4me2, AC-H3, cleavage caspase3/9, BAX, and p21 proteins were significantly increased by 4SC-202. (B) The mRNA levels of LSD1 and HDAC3 were detected by qRT-PCR, showing that the mRNA levels were suppressed after treatment with 0.7 μM 4SC-202 for 24 h. (C) Cells were exposed to 0.5 μM 4SC-202 for different time (0, 6, 12, 24, 48 h), and these above proteins were also detected by western blot and the result was similar with (A). (D, E) Next, Western blot and qRT-PCR analyzed that 4SC-202 treatment suppressed the expression levels of HO-1 in a drug-dependent manner. (F) Western blot also shown that 4SC-202 down-regulated the HO-1 protein level in a time-dependent manner. (G) Fluorescence microscopy was used to detect the transfection rate of cells after transfection with HO-1 overexpression lentivirus or its empty control vector. Green fluorescence represented the successful transfection of the virus. (H) qRT-PCR was used to detect mRNA levels of HO-1 after lentivirus transfection and confirmed the up-regulation of HO-1 expression level. (I) Western blot analyzed that up-regulation of HO-1 could significantly attenuate the 4SC-202-induced the levels of cleaved caspase3/9 and BAX proteins, meanwhile limit the 4SC-202-decreased the level of BCL-2 protein. (J, K) Flow cytometry was used to detect apoptotic rate, which was analyzed by GraphPad Primer 8 after the same treatment in (I). The result indicated that up-regulation of HO-1 could significantly attenuate the 4SC-202-induced the apoptotic rate. LV-HO-1 represented overexpression of HO-1; EV represented the control vector lentivirus. β-actin was used as an internal reference. All experiments were performed in triplicate. Dates were shown as mean ± SD. *, P<0.05 versus control; **, P<0.01 versus control; ***, P<0.001 versus control; and #, P>0.05 versus control. Statistical analysis was performed by the student's t test.

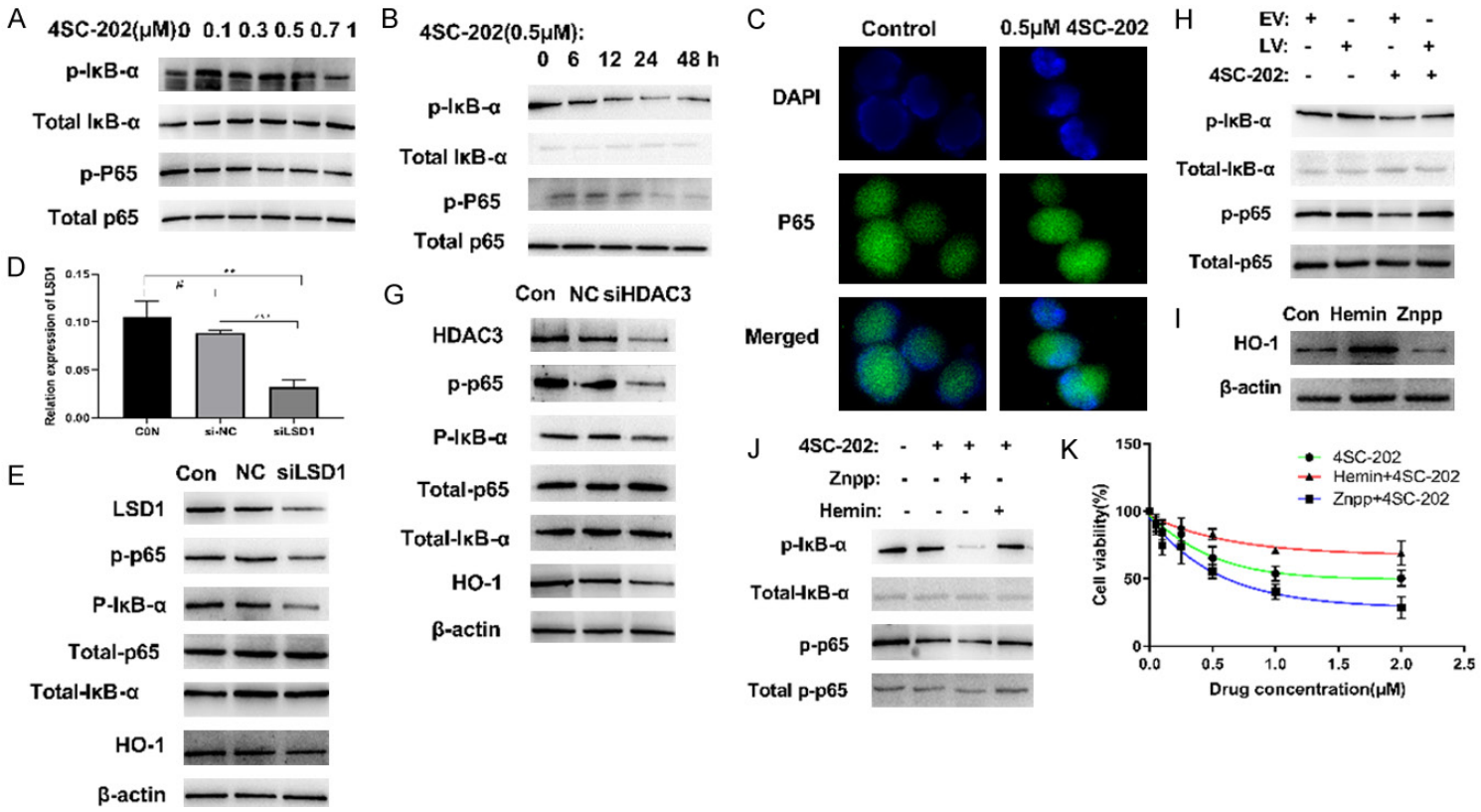

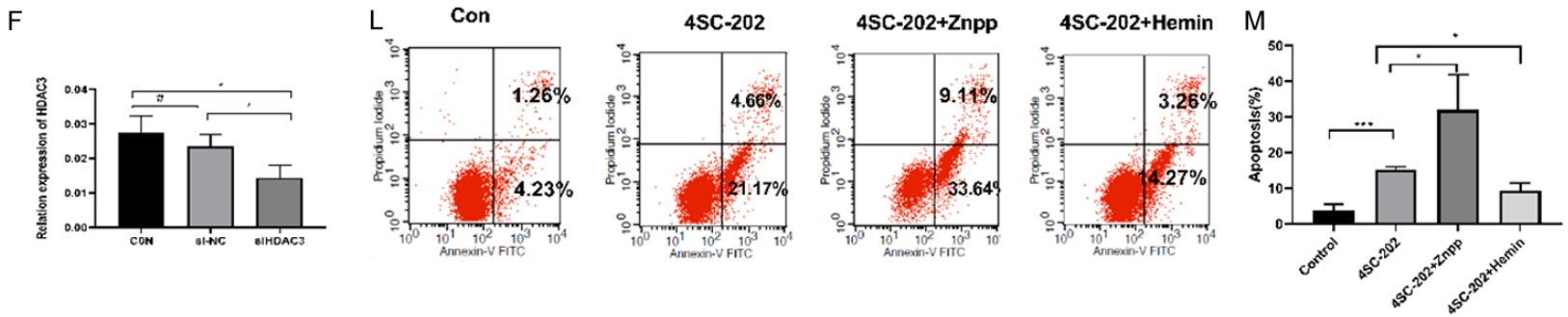

Figure 4. 4SC-202 induced apoptosis and down-regulated HO-1 expression via NF-κB, and HO-1 affected the efficacy of 4SC-202 in SKM-1 cells. (A, B) Western blot detected that 4SC-202 treatment inhibited the expression of p-p65 and p-Iκ-α but not total p65 and total IκB-α in SKM-1 cells. (C) Cells were exposed to 0.5 μM 4SC-202 for 24 h. The translocation of p65 was determined by immunofluorescence staining (original magnification, ×1,000). The merged images were obtained after superposition of the green (P65) and blue (DAPI) channels. The images are representative of 3 separate experiments. (D) siRNA targeting LSD1 was used for LSD1 silencing, followed by qRT-PCR to determine its transfection effect; siLSD1 represented siRNA targeting LSD1 and NC represented the negative control of siRNA. (E) After transfection siRNA targeting LSD1 for 48 h, Western blot analyzed that LSD1 inhibited the expression of p-P65, p-IκB-α, and HO-1 proteins but not total P65 and IκB-α. (F) siRNA targeting HDAC3 was used for HDAC3 silencing in cells, followed by qRT-PCR to determine its transfection effect. (G) Similarly, after transfection siRNA targeting HDAC3 for 48 h, western blot analysis shown that HDAC3 down-regulated the expression of p-P65, p-IκB-α, and HO-1 proteins but not total P65 and IκB-α in SKM-1 cells. (H) Cells were transfected with HO-1 lentivirus, and subsequently treated with or without 0.5 μM 4SC-202. Western blot detect the expression levels of NF-κB pathway-related protein. (I) After cells were treated with Znpp or Hemin for 24 h, Western blot analysis shown that the HO-1 protein level was decreased by Znpp while increased by Hemin. (J) After treatment with Znpp and Hemin with or without 0.5 μM 4SC-202 treatment for 24 h, western blot was subsequently used to analyze the expression of NF-κB pathway-related protein, showing that Znpp further decreased the protein levels of p-P65 and p-IκB-α, which were increased by Hemin. (K) CCK-8 assay also indicated that Znpp enhanced 4SC-202-induced cell viability attenuation, while Hemin partially reversed the efficacy of 4SC-202. (L, M) After the same treatment with (J), flow cytometry analysis suggested that Znpp enhanced 4SC-202-induced cell apoptotic rate ($P<0.05$), while Hemin partially reversed 4SC-202-induced apoptotic rate ($P<0.05$) in SKM-1 cells. Total P-65 and total IκB-α proteins were considered as the internal reference of the NF-κB pathway of p-p65 and p-IκB-α, respectively, and β-actin was used as a loading control. Dates were represented as mean ± SD. *, $P<0.05$; **, $P<0.01$; ***, $P<0.001$ and #, $P>0.5$. All experiments were repeated three times. Statistical analysis was performed by the student's t test.

by Western blot to detect the levels of NF-κB pathway proteins. As a result, up-regulation of HO-1 hardly affected the levels of NF-κB pathway protein levels, which significantly attenuated 4SC-202-induced down-regulation of p-p65 and p-IκB-α protein levels (**Figure 4H**).

Regulation of HO-1 affects the sensitivity of cancer cells against demethylation and other chemotherapy drugs [22, 25, 26, 31]. To further comprehensively determine how HO-1 affected the activity of 4SC-202, cells were treated with 10 μM Hemin (a HO-1 activator) or 0.05 μM Znpp (an inhibitor of HO-1), followed by Western blot to HO-1 protein level (**Figure 4I**). These treated cells were also treated with 0.5 μM 4SC-202. We found that Znpp further decreased the protein levels of p-P65 and p-IκB-α, which were increased by Hemin (**Figure 4J**). After co-incubation of 4SC-202 (0-4 μM) with Znpp or Hemin, CCK-8 assay showed that Znpp enhanced 4SC-202-induced cell viability attenuation, while Hemin partially reversed the efficacy of 4SC-202 (**Figure 4K**). Under the same condition, Znpp enhanced 4SC-202-induced cell apoptotic rate ($P<0.05$), while Hemin partially reversed 4SC-202-induced apoptotic rate ($P< 0.05$) in SKM-1 cells (**Figure 4L**, **4M**). Taken together, 4SC-202 can regulate HO-1 to induce apoptosis via NF-κB pathway, and HO-1 partially reversed the efficacy of 4SC-202 against SKM-1 cells.

HO-1 partially reversed the inhibitory effects of 4SC-202 on SKM-1 cell proliferation in vivo

Finally, SKM-1 cells transfected with LV-HO-1 and its empty vector (EV), were injected to the tail vein of NOD/SCID mice. After confirming successful engraftment in these recipient mice at 14 days after transplantation, 4SC-202 was orally administered at a dose of 80 mg/kg/day for five consecutive days, followed by observation of the change in human CD45-positive cells by flow cytometry. As a result, after 2 weeks of 4SC-202 administration, the proportion of human CD34-positive cells were significantly decreased, and we found that up-regulation of HO-1 accelerated cell proliferation and decreased the 4SC-202-inhibited MDS cell proliferation (**Figure 5A**, **5B**). Meanwhile, we observed for 130 days and recorded the death time of these mice, which was showed by Kaplan-Meier plot. The survival curve indicated that 4SC-202 effectively improved the survival of recipient mice, however, up-regulation of HO-1 delayed the time of 4SC-202-killing SKM-1 cells (**Figure 5C**). These results indicated that 4SC-202 effectively inhibited MDS cell proliferation and HO-1 influenced the inhibitory effects of 4SC-202 on SKM-1 cell proliferation in vivo.

Discussion

LSD1 blocks the differentiation of primary progenitor cells, promotes abnormal hematopoiesis and drives the progression in MDS and MDS-related leukemia [3]. Niebel D et al. have found that LSD1 was highly expressed in MDS and AML [2]. Similarly, here, we also found the high expression of LSD1 in bone marrow from MDS/AML patients compared with healthy controls. LSD1 is associated with HDAC1/2, and they formed a co-inhibitor to abnormally inhibit some transcriptional genes, thereby repressing DNA complication. Previous clinical trials have shown that HDAC inhibitors are less effective in treating MDS patients; and even if HDAC inhibitors are combined with decitabine, the efficacy of decitabine is not improved in MDS patients [15]. However, in this study, co-inhibition of LSD1 and HDACs exerted strong efficacy against SKM-1 cells. 4SC-202 is a dual inhibitor against LSD1 and HDAC1/2/3. Wobser M et al. have reported that 4SC-202 has the potential to inhibit cancer cell growth independent of targeting these epigenetic modifiers, and independent of altering cellular transcription [19]. 4SC-202 hardly decreased the expression of LSD1 in melanoma [16, 32-34].

We found that 4SC-202 or silencing LSD1 or HDAC3 by siRNA could down-regulate the expression of HO-1 and inhibited the activation of NF-κB pathway. In this study, up-regulation of HO-1 attenuated 4SC-202-induce apoptosis. Except for cleaved caspase9, HO-1 hardly directly regulated NF-κB pathway and other related-apoptotic proteins, whereas HO-1 could significantly attenuated 4SC-202-induced down-regulation of BCL-2 protein, up-regulation of cleaved caspase3/9 proteins and suppressed activation of NF-κB pathway. It is reported that HO-1 affects the sensitivity of cancer cells against demethylation and others chemotherapy drugs. To further comprehensively determine how HO-1 affected the activity of 4SC-202, cells were treated with Hemin or Znpp. When Znpp down-regulated HO-1 expression, 4SC-202-induced cell apoptotic rate was significantly increased. However, 4SC-202-induced apoptosis was clearly decreased by Hemin. HO-1 decreased the sensitivity of 4SC-202 against MDS cells, in turn a lack of HO-1 in-

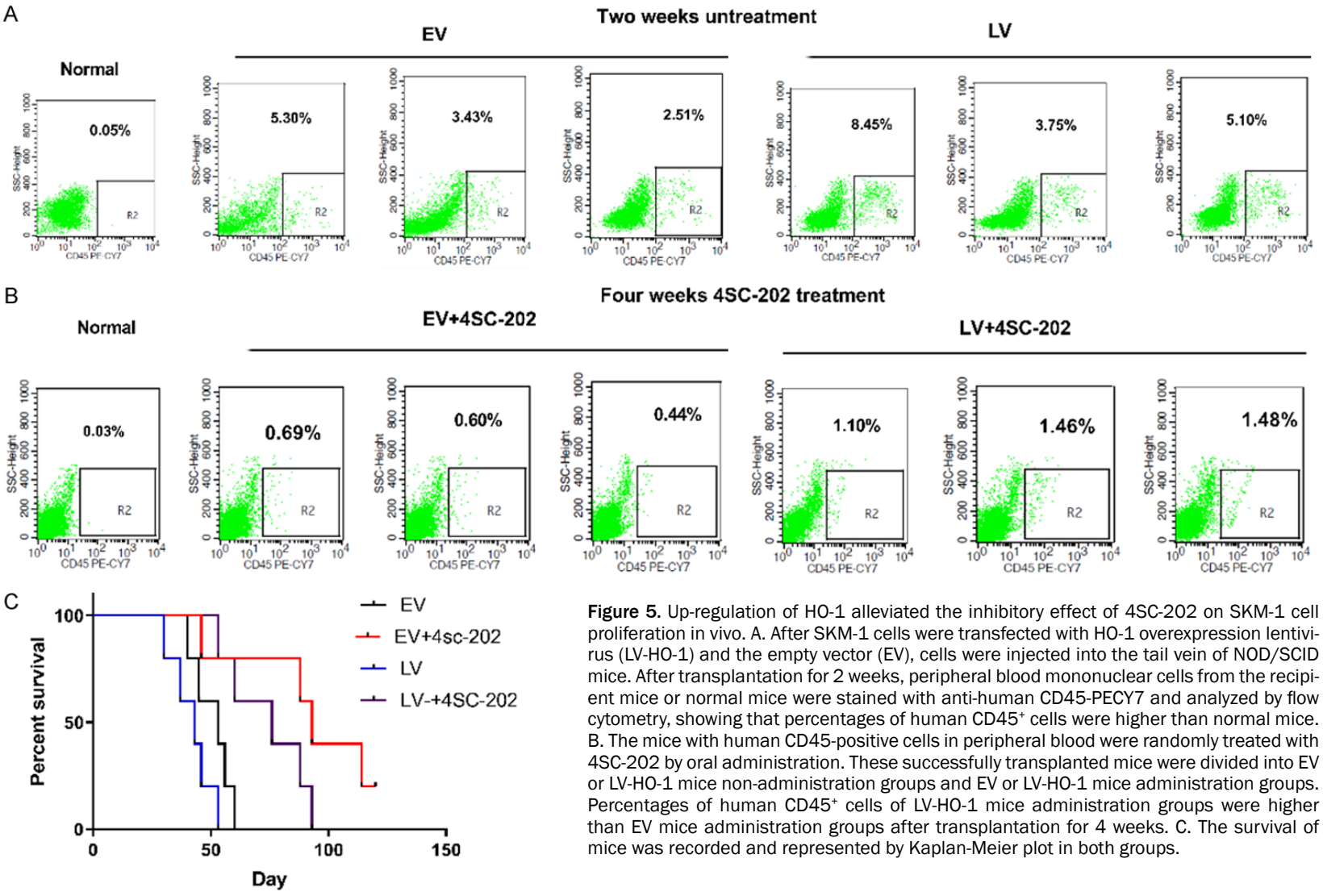

Figure 5. Up-regulation of HO-1 alleviated the inhibitory effect of 4SC-202 on SKM-1 cell proliferation in vivo. A. After SKM-1 cells were transfected with HO-1 overexpression lentivirus (LV-HO-1) and the empty vector (EV), cells were injected into the tail vein of NOD/SCID mice. After transplantation for 2 weeks, peripheral blood mononuclear cells from the recipient mice or normal mice were stained with anti-human CD45-PECY7 and analyzed by flow cytometry, showing that percentages of human $CD45^+$ cells were higher than normal mice. B. The mice with human CD45-positive cells in peripheral blood were randomly treated with 4SC-202 by oral administration. These successfully transplanted mice were divided into EV or LV-HO-1 mice non-administration groups and EV or LV-HO-1 mice administration groups. Percentages of human $CD45^+$ cells of LV-HO-1 mice administration groups were higher than EV mice administration groups after transplantation for 4 weeks. C. The survival of mice was recorded and represented by Kaplan-Meier plot in both groups.

creased the sensitivity of 4SC-202-induced repressed activity of NF-κB pathway in SKM-1 cells. Taken together, these results indicated that the 4SC-202 could mediated HO-1-induced apoptosis via NF-κB pathway, and HO-1 influenced the effects of 4SC-202.

Next, we evaluated the therapeutic effect of 4SC-202 under the influence of HO-1 in vivo. After SKM-1 cells were transfected with LV-HO-1 and its empty vector (EV), cells were injected into the tail vein of NOD/SCID mice. Two weeks after transplantation, we determined if these mice were successfully transplanted. The successfully transplanted mice into were divided into EV or LV-HO-1 mice non-administration groups, EV or LV-HO-1 mice administration groups. Human $CD45^+$ content of mice from the 4SC-202 administrator groups were detected by flow cytometry two weeks after administration. As a result, $CD45^+$ cells were gradually decreased over time, consistent with the result of Sugino et al. [3], which suggested that up-regulation of HO-1 delayed the time of 4SC-202-killing SKM-1 cells. In addition, 4SC-202 improved survival rate while HO-1 decreased survival rate in MDS mice. These results have demonstrated that 4SC-202 is a potent inhibitor of poor prognosis in MDS, which also further confirms the mechanism of 4SC-202.

Collectively, 4SC-202, an inhibitor of LSD1 and HDAC1/2/3, significantly inhibited cell growth by causing cell cycle arrest at G2/M, inducing apoptosis and decreasing HO-1 gene expression via the suppression of NF-κB pathway in MDS cells. In addition, up-regulation of HO-1 expression attenuated the inhibitory effect of 4SC-202-induced activation of NF-κB pathway, thereby attenuating the efficacy of 4SC-202, but low HO-1 expression enhanced the efficacy of 4SC-202in MDS cells. Hopefully, the present study could provide a novel therapeutic strategy in MDS.

Acknowledgements

This study was supported by the National Natural Science Foundation of China (No. 8166-0616, 81960032), Guizhou Province Key Clinical Subject Construction Project and Guizhou Province Science and Technology Department Project (No. qiankehe [2018]4618). We thanked Hematopoietic Stem Cell Laboratory, Guizhou Medical University for providing clinical samples.

Disclosure of conflict of interest

None.

Address correspondence to: Dr. Qin Fang, Department of Pharmacy, The Affiliated Hospital of Guizhou Medical University, Guiyang, Guizhou, P. R. China. Tel: +86-0851-86774149; Fax: +86-0851-86774-149; E-mail: 1731998914@qq.com; Dr. Jishi Wang, Department of Hematology, The Affiliated Hospital of Guizhou Medical University, Guiyang, P. R. China. Tel: +86-0851-86774149; Fax: +86-0851-8677-4149; E-mail: wangjishi9646@163.com

References

[1] Sperling AS, Gibson CJ and Ebert BL. The genetics of myelodysplastic syndrome: from clonal haematopoiesis to secondary leukaemia. Nat Rev Cancer 2017; 17: 5-19.

[2] Niebel D, Kirfel J, Janzen V, Holler T, Majores M and Gutgemann I. Lysine-specific demethylase 1 (LSD1) in hematopoietic and lymphoid neoplasms. Blood 2014; 124: 151-152.

[3] Sugino N, Kawahara M, Tatsumi G, Kanai A, Matsui H, Yamamoto R, Nagai Y, Fujii S, Shimazu Y, Hishizawa M, Inaba T, Andoh A, Suzuki T and Takaori-Kondo A. A novel LSD1 inhibitor NCD38 ameliorates MDS-related leukemia with complex karyotype by attenuating leukemia programs via activating super-enhancers. Leukemia 2017; 31: 2303-2314.

[4] Castelli G, Pelosi E and Testa U. Targeting histone methyltransferase and demethylase in acute myeloid leukemia therapy. Onco Targets Ther 2018; 11: 131-155.

[5] Magliulo D, Bernardi R and Messina S. Lysine-specific demethylase 1A as a promising target in acute myeloid leukemia. Front Oncol 2018; 8: 255.

[6] Schenk T, Chen WC, Gollner S, Howell L, Jin L, Hebestreit K, Klein HU, Popescu AC, Burnett A, Mills K, Casero RA Jr, Marton L, Woster P, Minden MD, Dugas M, Wang JC, Dick JE, Muller-Tidow C, Petrie K and Zelent A. Inhibition of the LSD1 (KDM1A) demethylase reactivates the all-trans-retinoic acid differentiation pathway in acute myeloid leukemia. Nat Med 2012; 18: 605-611.

[7] Mould DP, McGonagle AE, Wiseman DH, Williams EL and Jordan AM. Reversible inhibitors of LSD1 as therapeutic agents in acute myeloid leukemia: clinical significance and progress to date. Med Res Rev 2015; 35: 586-618.

[8] Ishikawa Y, Nakayama K, Morimoto M, Mizutani A, Nakayama A, Toyoshima K, Hayashi A, Takagi S, Dairiki R, Miyashita H, Matsumoto S, Gamo K, Nomura T and Nakamura K. Synergistic anti-AML effects of the LSD1 inhibitor

T-3775440 and the NEDD8-activating enzyme inhibitor pevonedistat via transdifferentiation and DNA rereplication. Oncogenesis 2017; 6: e377.

[9] Shi Y, Lan F, Matson C, Mulligan P, Whetstine JR, Cole PA, Casero RA and Shi Y. Histone demethylation mediated by the nuclear amine oxidase homolog LSD1. Cell 2004; 119: 941-953.

[10] Hojfeldt JW, Agger K and Helin K. Histone lysine demethylases as targets for anticancer therapy. Nat Rev Drug Discov 2013; 12: 917-930.

[11] Maiques-Diaz A, Spencer GJ, Lynch JT, Ciceri F, Williams EL, Amaral FMR, Wiseman DH, Harris WJ, Li Y, Sahoo S, Hitchin JR, Mould DP, Fairweather EE, Waszkowycz B, Jordan AM, Smith DL and Somervaille TCP. Enhancer activation by pharmacologic displacement of LSD1 from GFI1 induces differentiation in acute myeloid leukemia. Cell Rep 2018; 22: 3641-3659.

[12] Forneris F, Binda C, Dall'Aglio A, Fraaije MW, Battaglioli E and Mattevi A. A highly specific mechanism of histone H3-K4 recognition by histone demethylase LSD1. J Biol Chem 2006; 281: 35289-35295.

[13] Maes T, Mascaró C, Tirapu I, Estiarte A, Ciceri F, Lunardi S, Guibourt N, Perdones A, Lufino MMP, Somervaille TCP, Wiseman DH, Duy C, Melnick A, Willekens C, Ortega A, Martinell M, Valls N, Kurz G, Fyfe M, Castro-Palomino JC and Buesa C. ORY-1001, a potent and selective covalent KDM1A inhibitor, for the treatment of acute leukemia. Cancer Cell 2018; 33: 495-511, e412.

[14] Fiskus W, Sharma S, Shah B, Portier BP, Devaraj SG, Liu K, Iyer SP, Bearss D and Bhalla KN. Highly effective combination of LSD1 (KDM1A) antagonist and pan-histone deacetylase inhibitor against human AML cells. Leukemia 2014; 28: 2155-2164.

[15] Heuser M, Yun H and Thol F. Epigenetics in myelodysplastic syndromes. Semin Cancer Biol 2018; 51: 170-179.

[16] Kalin JH, Wu M, Gomez AV, Song Y, Das J, Hayward D, Adejola N, Wu M, Panova I, Chung HJ, Kim E, Roberts HJ, Roberts JM, Prusevich P, Jeliazkov JR, Roy Burman SS, Fairall L, Milano C, Eroglu A, Proby CM, Dinkova-Kostova AT, Hancock WW, Gray JJ, Bradner JE, Valente S, Mai A, Anders NM, Rudek MA, Hu Y, Ryu B, Schwabe JWR, Mattevi A, Alani RM and Cole PA. Targeting the CoREST complex with dual histone deacetylase and demethylase inhibitors. Nat Commun 2018; 9: 53.

[17] Pinkerneil M, Hoffmann MJ, Kohlhof H, Schulz WA and Niegisch G. Evaluation of the therapeutic potential of the novel isotype specific HDAC inhibitor 4SC-202 in urothelial carcinoma cell lines. Target Oncol 2016; 11: 783-798.

[18] von Tresckow B, Sayehli C, Aulitzky WE, Goebeler ME, Schwab M, Braz E, Krauss B, Krauss R, Hermann F, Bartz R and Engert A. Phase I study of domatinostat (4SC-202), a class I histone deacetylase inhibitor in patients with advanced hematological malignancies. Eur J Haematol 2019; 102: 163-173.

[19] Wobser M, Weber A, Glunz A, Tauch S, Seitz K, Butelmann T, Hesbacher S, Goebeler M, Bartz R, Kohlhof H, Schrama D and Houben R. Elucidating the mechanism of action of domatinostat (4SC-202) in cutaneous T cell lymphoma cells. J Hematol Oncol 2019; 12: 30.

[20] Salerno L, Romeo G, Modica MN, Amata E, Sorrenti V, Barbagallo I and Pittala V. Heme oxygenase-1: a new druggable target in the management of chronic and acute myeloid leukemia. Eur J Med Chem 2017; 142: 163-178.

[21] Sorrenti V, Pittala V, Romeo G, Amata E, Dichiara M, Marrazzo A, Turnaturi R, Prezzavento O, Barbagallo I, Vanella L, Rescifina A, Floresta G, Tibullo D, Di Raimondo F, Intagliata S and Salerno L. Targeting heme Oxygenase-1 with hybrid compounds to overcome Imatinib resistance in chronic myeloid leukemia cell lines. Eur J Med Chem 2018; 158: 937-950.

[22] Ma D, Fang Q, Wang P, Gao R, Sun J, Li Y, Hu XY and Wang JS. Downregulation of HO-1 promoted apoptosis induced by decitabine via increasing p15INK4B promoter demethylation in myelodysplastic syndrome. Gene Ther 2015; 22: 287-296.

[23] Wang P, Ma D, Wang J, Fang Q, Gao R, Wu W, Lu T and Cao L. Silencing HO-1 sensitizes SKM-1 cells to apoptosis induced by low concentration 5-azacytidine through enhancing p16 demethylation. Int J Oncol 2015; 46: 1317-1327.

[24] Cheng B, Tang S, Zhe N, Ma D, Yu K, Wei D, Zhou Z, Lu T, Wang J and Fang Q. Low expression of GFI-1 Gene is associated with Panobinostat-resistance in acute myeloid leukemia through influencing the level of HO-1. Biomed Pharmacother 2018; 100: 509-520.

[25] Wei D, Lu T, Ma D, Yu K, Li X, Chen B, Xiong J, Zhang T and Wang J. Heme oxygenase-1 reduces the sensitivity to imatinib through nonselective activation of histone deacetylases in chronic myeloid leukemia. J Cell Physiol 2019; 234: 5252-5263.

[26] Tang S, Cheng B, Zhe N, Ma D, Xu J, Li X, Guo Y, Wu W and Wang J. Histone deacetylase inhibitor BG45-mediated HO-1 expression induces apoptosis of multiple myeloma cells by the JAK2/STAT3 pathway. Anticancer Drugs 2018; 29: 61-74.

[27] Huang J, Guo P, Ma D, Lin X, Fang Q and Wang J. Overexpression of heme oxygenase-1 induced by constitutively activated NF-kappaB

as a potential therapeutic target for activated B-cell-like diffuse large B-cell lymphoma. Int J Oncol 2016; 49: 253-264.
[28] Braun T, Carvalho G, Coquelle A, Vozenin MC, Lepelley P, Hirsch F, Kiladjian JJ, Ribrag V, Fenaux P and Kroemer G. NF-kappaB constitutes a potential therapeutic target in high-risk myelodysplastic syndrome. Blood 2006; 107: 1156-1165.
[29] Seifermann M and Epe B. Oxidatively generated base modifications in DNA: not only carcinogenic risk factor but also regulatory mark? Free Radic Biol Med 2017; 107: 258-265.
[30] Kim D, Nam HJ, Lee W, Yim HY, Ahn JY, Park SW, Shin HR, Yu R, Won KJ, Bae JS, Kim KI and Baek SH. PKCalpha-LSD1-NF-kappaB-signaling cascade is crucial for epigenetic control of the inflammatory response. Mol Cell 2018; 69: 398-411, e396.
[31] Wei S, Wang Y, Chai Q, Fang Q, Zhang Y and Wang J. Potential crosstalk of Ca2+-ROS-dependent mechanism involved in apoptosis of Kasumi-1 cells mediated by heme oxygenase-1 small interfering RNA. Int J Oncol 2014; 45: 2373-2384.
[32] Mishra VK, Wegwitz F, Kosinsky RL, Sen M, Baumgartner R, Wulff T, Siveke JT, Schildhaus HU, Najafova Z, Kari V, Kohlhof H, Hessmann E and Johnsen SA. Histone deacetylase class-I inhibition promotes epithelial gene expression in pancreatic cancer cells in a BRD4- and MYC-dependent manner. Nucleic Acids Res 2017; 45: 6334-6349.
[33] Fu M, Wan F, Li Z and Zhang F. 4SC-202 activates ASK1-dependent mitochondrial apoptosis pathway to inhibit hepatocellular carcinoma cells. Biochem Biophys Res Commun 2016; 471: 267-273.
[34] Gruber W, Peer E, Elmer DP, Sternberg C, Tesanovic S, Del Burgo P, Coni S, Canettieri G, Neureiter D, Bartz R, Kohlhof H, Vitt D and Aberger F. Targeting class I histone deacetylases by the novel small molecule inhibitor 4SC-202 blocks oncogenic hedgehog-GLI signaling and overcomes smoothened inhibitor resistance. Int J Cancer 2018; 142: 968-975.